

## 28. INORGANIC GEOCHEMISTRY OF SEDIMENTS AND ROCKS FROM THE MID-PACIFIC MOUNTAINS AND HESS RISE, DEEP SEA DRILLING PROJECT LEG 62<sup>1</sup>

Walter E. Dean, U.S. Geological Survey, Denver, Colorado

### INTRODUCTION

A total of 191 samples was collected for inorganic geochemical analyses from DSDP Holes 463, 464, 465, 465A, and 466. These samples were collected with two main goals. First, at least one sample was collected from each core, whenever possible, to document the general geochemical variability within lithologic units. Unfortunately, several lithologic units were inadequately sampled because of poor recovery, mostly due to the presence of chert. The least-sampled units are Units III in Hole 464 and Units IB and II in Hole 466. The second goal was to look for geochemical differences between contrasting lithologies within main lithologic units, particularly between cyclic interbeds of red and green limestone in Lithologic Unit II, Hole 463, and between olive, laminated limestone and gray, massive limestone in Lithologic Unit II, Hole 465A.

### METHODS

The 191 geochemical samples were analyzed for 30 major, minor, and trace elements using semiquantitative optical emission spectroscopy, X-ray fluorescence, and atomic-absorption spectrophotometry. Two elements (Be and Pb) were detected only in samples from Hole 464. Details of the analytical methods are described in the analytical sections of the report by Miesch (1976). Twenty-four of the 191 samples were chosen at random for duplicate analyses; all 215 analytical samples (191 samples plus 24 duplicates) were submitted in a random sequence to the analytical laboratories of the U.S. Geological Survey.

Samples were air-dried and ground in a ceramic mill to pass a 100-mesh (149  $\mu\text{m}$ ) sieve. Because the samples were air-dried, concentrations of Na and Mg are too high, owing to  $\text{Na}^+$  and  $\text{Mg}^{+2}$  dissolved in interstitial water and left as a residue after evaporation. To correct these values, I assumed that all the Cl determined by X-ray fluorescence was due to  $\text{Cl}^-$  dissolved in the interstitial water, and that this water contained the same proportions of  $\text{Na}^+$ ,  $\text{Mg}^{+2}$ , and  $\text{Cl}^-$  as average sea water. Contributions of Mg and Na from interstitial water were then subtracted from the analytical values.

### RESULTS

#### Site 463

Results of analyses of 106 samples (including nine analytical duplicates) from Hole 463 are given in Table 1 and plotted versus sub-bottom depth in Figure 1.

Lithologic Unit I consists of foraminifer and nannofossil ooze and chalk. Concentrations of  $\text{CaCO}_3$  range from about 70 to 100%, but concentrations in most samples are greater than 90% (Site 463 report, this

volume). Silicification of chalk associated with chert occurs below Core 30, and this is indicated by higher Si concentrations in some samples (Fig. 1). The most notable chemical characteristics of the ooze and chalk in Unit I are the relatively high concentrations of Ba (average of about 1200 ppm) and Sr (range of about 1000 to 3000 ppm). Concentrations of Sr decrease steadily with depth, from about 3000 ppm (0.3%) or more near the sediment/water interface to about 500 ppm in limestones in Units II, III, and IV. I interpret this decrease with depth to represent progressive loss of Sr during diagenesis. Wangersky and Joensuu (1964, 1967) reported average values of Sr ranging from 1500 to 1700 ppm in coarse fractions ( $>62 \mu\text{m}$ ) of samples from five deep-sea carbonate cores from the Atlantic and Caribbean. Average values of Sr in the fine fractions from the same 5 cores ranged from 1900 to 2300 ppm. Turekian (1964) reported an average concentration of 1200 ppm Sr in foraminifer  $\text{CaCO}_3$ . Samples from Hole 463, therefore, appear to be higher in Sr than expected in ooze (Unit IA), and lower than expected in limestone.

Unit II consists of cyclic interbeds of greenish-gray limestone with gray, white, or red limestone. All the limestones show varying degrees of silicification, indicated by variations in the concentration of Si (Fig. 1). The most pronounced color difference is between the greenish-gray and reddish- or pinkish-gray limestones in Cores 57 through 65 (Fig. 2). Chemical differences between green and red limestones will be discussed later.

Unit III consists of limestone similar to the multi-colored limestones in Unit II, with the addition of beds of tuff-rich limestone and (in Cores 70 and 71), organic-carbon-rich limestone that contains up to 4% organic carbon (Dean et al., this volume). A considerable amount of silicification occurs in all the limestones in Unit III, especially in the organic-carbon-rich limestones (Fig. 1). Most elements show a greater range of variability between samples of limestone from both Units II and III relative to element variability within overlying and underlying units. This is particularly evident for Si, Al, K, Ti, B, Ba, Cr, Cu, Mn, Zn, and Zr.

Summary statistics for analyses of 18 samples of red limestone and 16 samples of green limestone from Unit II (Cores 57-64, 500 to 560 m sub-bottom) are given in Table 2 and plotted in Figure 3. These samples are indicated in Table 1 by "g" (green) and "r" (red) following the interval designation for samples. It is apparent from Table 2 and Figure 3 that the red limestones contain higher concentrations of most elements than the

<sup>1</sup> Initial Reports of the Deep Sea Drilling Project, Volume 62.





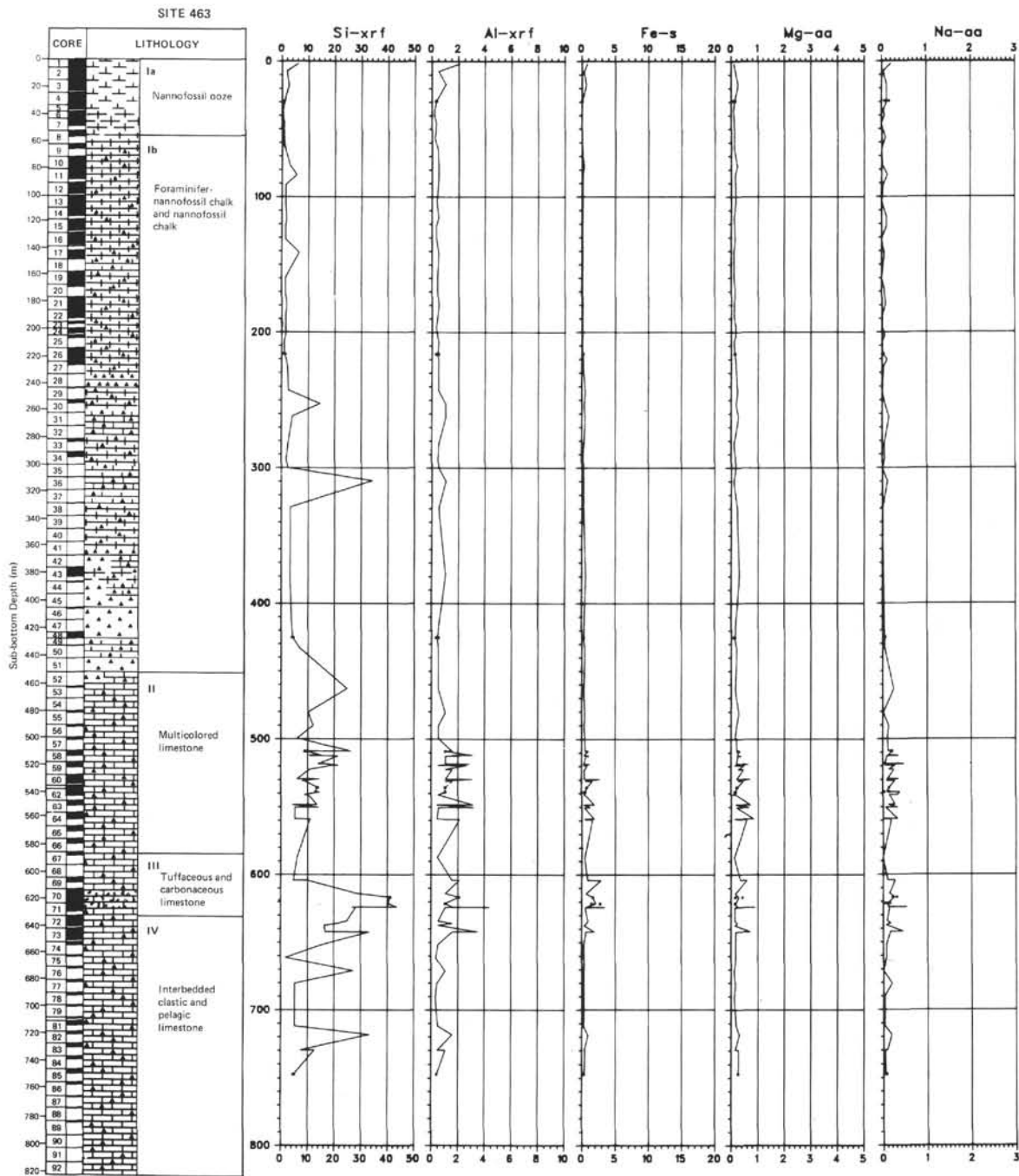


Figure 1. Lithologic summary and plots of element concentrations in samples from Hole 463. Element concentrations are in percent (unlabeled) or parts per million (labeled ppm) dry weight. Analyses were by X-ray fluorescence (xrf), semiquantitative optical emission spectroscopy (s), or atomic absorption spectrophotometry (aa). Duplicate analyses are indicated by two points connected by a horizontal bar at the same depth. The thickness of the black interval beside each core number in the column labeled "core" indicates the proportion of the cored interval that was recovered.

green limestones. These differences appear to be greatest in limestone samples from Cores 60 through 64 (Table 1), and for Fe, Mg, Na, Ti, Co, Cr, Cu, Ni, and V. There are no differences in concentrations of Si and Al between red and green limestones that would indicate that one or the other contained more clay minerals. Therefore, I interpret the higher element concentrations in the red limestones to be the result of greater adsorp-

tion by hydrous ferric oxides which I assume give the red limestones their distinctive color.

**Site 464**

Results of analyses of 15 samples (including four analytical duplicates) from Hole 464 are given in Table 3 and plotted versus sub-bottom depth in Figure 4. Twelve of these 15 samples are from brown clay, and

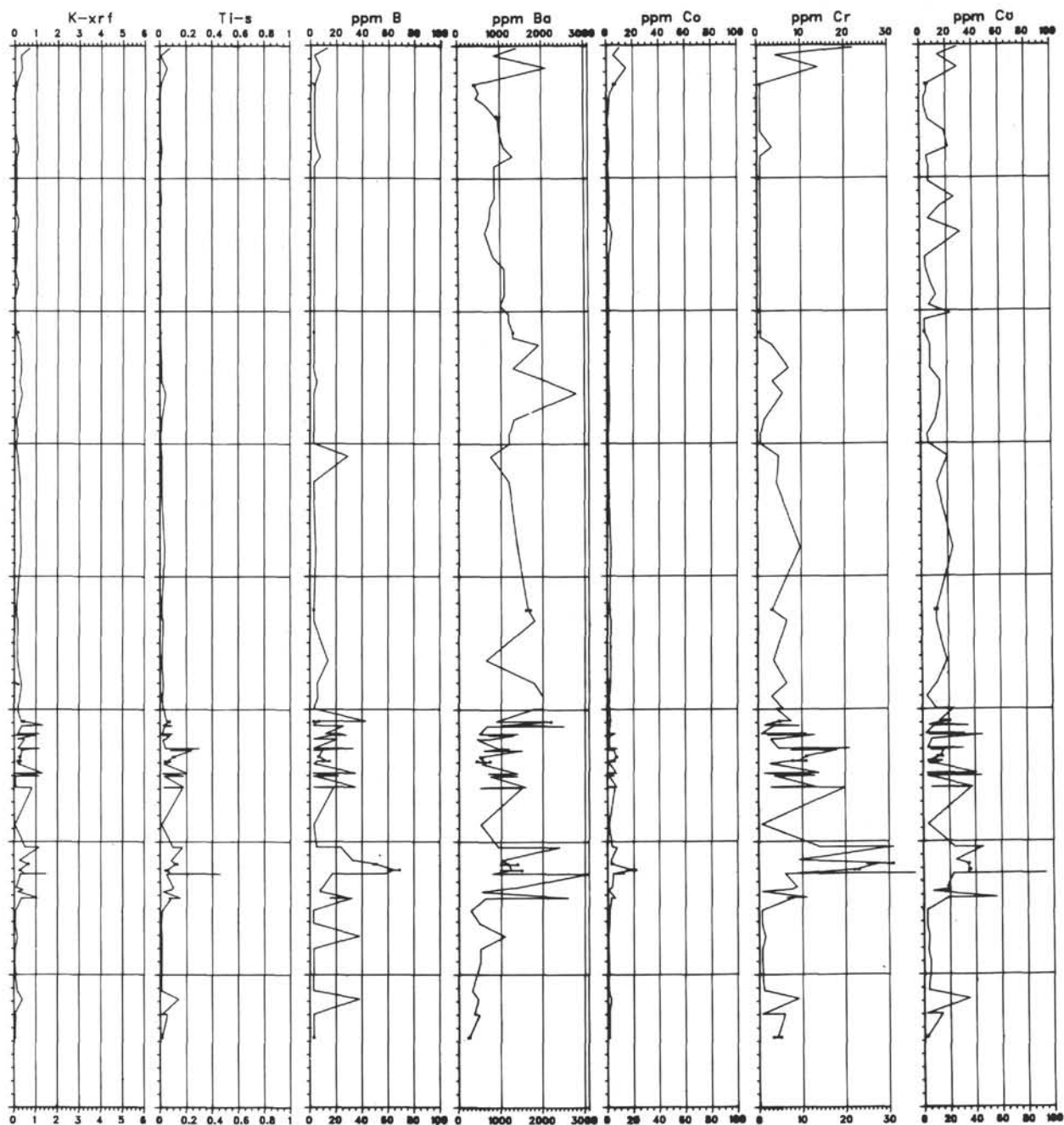


Figure 1. (Continued).

summary statistics for these samples are given in Table 4. Because Site 464 is below the carbonate-compensation depth, and apparently has been at least since the Miocene, there is no carbonate dilution of pelagic clays. This brown pelagic clay contains especially high concentrations of Fe and Mn due to hydrated oxides of Fe and Mn, which are known to be effective scavengers of trace metals, particularly Ni, Cu, Co, Zn—and to a lesser extent Cr, Mo, Ba, and Pb (e.g., Burns and Brown, 1972; Varentsov and Pronina, 1973; Burns and Burns, 1977).

The combination of no carbonate dilution and trace-metal scavenging results in higher concentrations of most elements relative to carbonate samples from the other three sites.

#### Site 465

Results of analyses of 62 samples (including six analytical duplicates) from Holes 465 and 465A are given in Table 5 and plotted versus sub-bottom depth in Figure 5. Unit I consists of white nannofossil ooze or

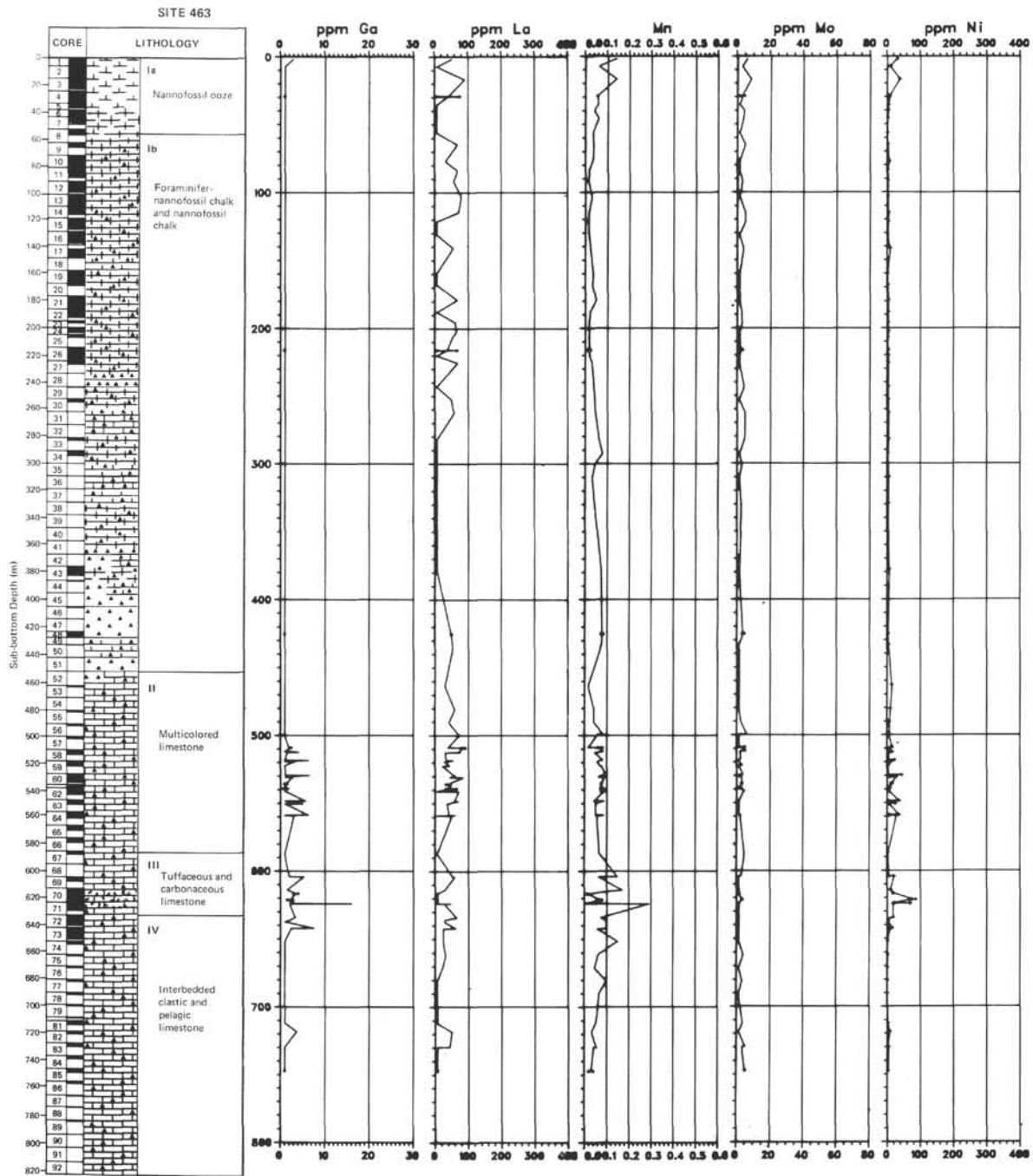


Figure 1. (Continued).

foraminifer-nannofossil ooze. Concentrations of  $\text{CaCO}_3$  range from 81 to 96%, but concentrations in most samples are greater than 90% (Site 465 report, this volume). Blebs of pyrite in Core 3A (62 meters sub-bottom) smeared into the ooze by the coring process have imparted an overall gray color to the ooze. These pyrite concentrations are associated with higher concentrations of a number of elements in samples from this depth. There are actually three samples collected between 61.88 and 62.64 meters sub-bottom that represent a transition from ooze to ooze with high concentrations

of pyrite. The geochemical gradient represented by these three samples is evident in Figure 5 and Table 5.

The concentrations of Sr decrease from about 3000 ppm (0.03%) at the sediment/water interface, to about 2000 ppm in samples of ooze, to an average of about 1000 ppm in samples of limestone from Unit II. This decrease in Sr with depth is more gradual and not as pronounced as in Hole 463 (Fig. 1). Concentrations of Ba in ooze from Hole 465 and 465A are also high (average of about 740 ppm), but not as high as in ooze and chalk from Hole 463 (average of about 1200 ppm).

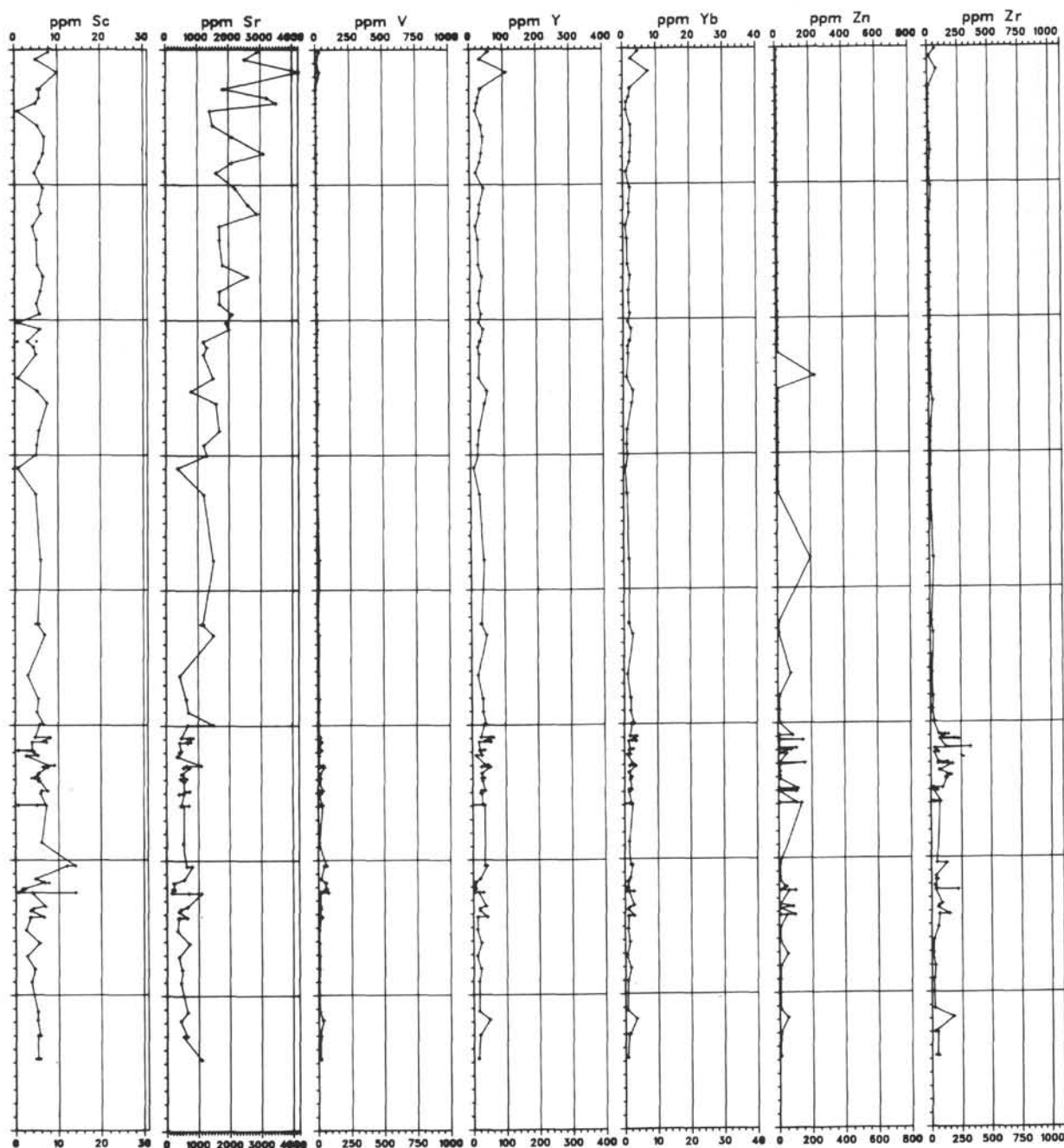


Figure 1. (Continued).

The dominant lithology of Unit II in Hole 465A is olive-gray laminated limestone (Fig. 6) that contains up to 8.6% organic carbon (Dean et al., this volume).

Most samples of olive limestone contain between 80 and 90%  $\text{CaCO}_3$ . This unit also contains rare to common interbeds of gray, massive to faintly laminated limestone (Fig. 6) that make up about 5% of the total thickness of Unit II (Site 465 report, this volume).

Summary statistics for analyses of 5 samples of gray massive limestone and 24 samples of olive laminated limestone from Unit II are given in Table 6 and plotted

in Figure 7. Samples of gray limestone are indicated by arrows on the plot for Si in Figure 5, and by a "g" following the interval designation for samples in Table 5; olive-gray limestone samples are indicated by "ol" following the interval designation in Table 5. The variability in concentrations of Si, evident in Figure 5, is due mainly to the higher degree of silicification of gray limestone relative to olive limestone (Table 6; Figure 7), although even the gray limestones are considerably less silicified than limestones in Units II and III in Hole 463 (Fig. 1).

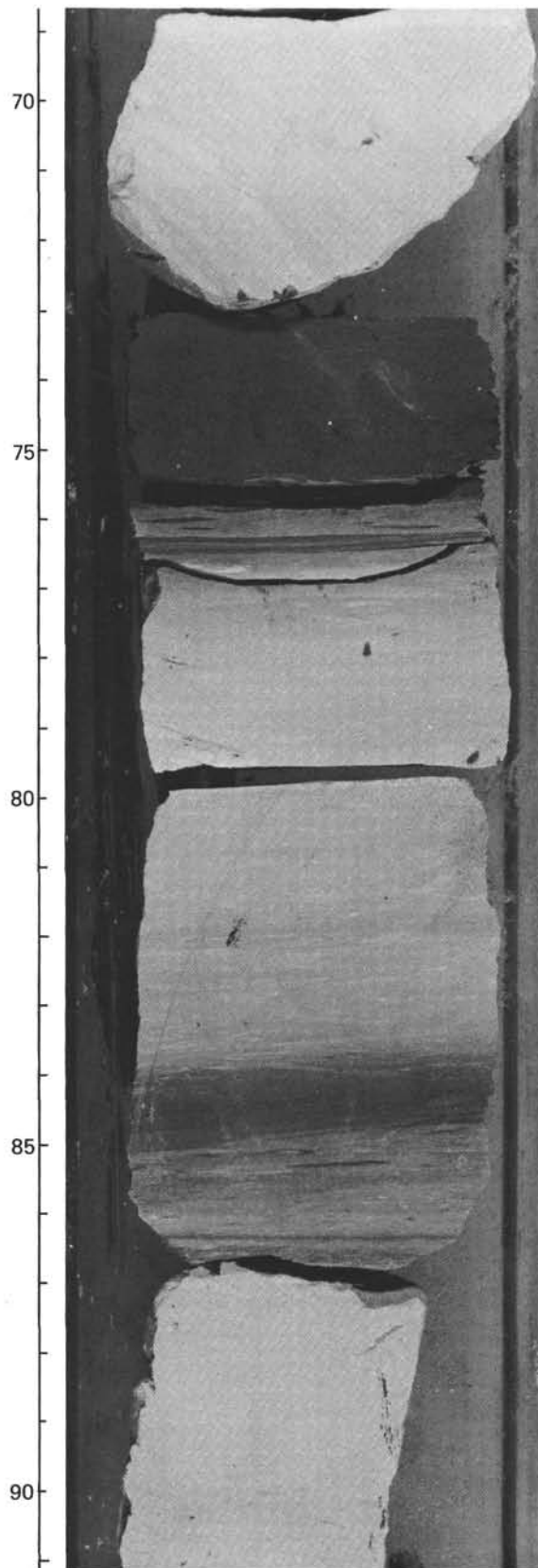


Figure 2. Interbeds of pinkish- or reddish-gray (dark) and greenish-gray (light) limestone from Lithologic Unit II, 463-67-2, 70-90 cm. Subdivisions on scale are in millimeters.

Table 2. Summary statistics for element concentrations in 18 samples of red limestone and 16 samples of green limestone from Lithologic Unit II, Hole 463.

Element	Red Limestone			Green Limestone		
	Observed Range	Arithmetic Mean	Standard Deviation	Observed Range	Arithmetic Mean	Standard Deviation
Si (%)	5.1-19	12	3.3	4.3-26	12	6.6
Al	<0.42-3.2	1.6	0.91	<0.42-3.1	1.1	0.80
Fe	0.41-2.7	1.1	0.62	0.34-1.2	0.53	0.20
Mg	0.19-0.84	0.42	0.21	0.075-0.65	0.22	0.13
Na	0.11-0.38	0.24	0.085	0.024-0.48	0.12	0.12
K	0.08-1.3	0.56	0.39	<0.017-1.3	0.33	0.38
Ti	<0.013-0.22	0.079	0.063	<0.013-0.18	0.040	0.023
Ba (ppm)	430-2500	1300	650	420-2000	820	390
Co	1.2-7.5	3.9	2.5	0.70-6.1	2.2	1.6
Cr	2.8-21	10	5.8	0.70-11	5.0	3.3
Cu	6.7-46	24	13	2.5-38	9.5	10
La	23-91	57	21	<7.0-73	45	21
Li	<7.0-13	7.9	1.9	<7.0-13	7.4	1.5
Mn	410-900	690	142	170-930	700	190
Mo	<1.5-4.9	2.4	1.1	<1.5-6.3	2.7	1.7
Ni	2.2-43	17	12	2.3-23	7.2	5.4
Sc	2.5-9.1	6.3	1.6	<0.7-7.5	4.8	1.9
Sr	330-850	550	140	420-1500	650	290
V	6.4-48	22	12	6.9-29	13	5.9
Y	11-65	37	15	<1.0-43	28	10
Yb	0.94-3.8	2.3	0.88	0.10-3.0	1.8	0.68
Zr	29-230	100	58	19-330	89	80

Relative to the olive limestones, the gray limestones also contain 10 times more Ba, as much as five times more Na, Ti, and Zr, and 2 to 4 times more Al, Fe, Mg, K, La, and Li. Compositions of the gray limestones also tend to be less variable than those of the olive limestones. Relative to the gray limestones, the olive limestones tend to contain higher concentrations of the transition elements, especially Cu (5 times higher), Ni (5 times higher), Cr, Mn, Mo, and V. The olive limestones also contain about twice as much Sr as the gray limestone; this difference is probably due to less dilution of Sr-bearing carbonate by silica.

Some trace-element enrichment in the organic-carbon-rich olive limestones may be due to concentration of these elements in organic matter. The association of certain trace elements—especially Cu, Zn, Mo, V, Ni, Cr, Ba, and Pb—with organic-carbon-rich sediments and rocks has been reported by many investigators (e.g., Wedepohl, 1964; Brongersma-Sanders, 1965; Calvert and Price, 1970; Vine and Tourtelot, 1970; Volkov and Fomina, 1974; Chester, et al., 1978, to name only a few).

The association of organic matter and high trace-element concentrations is usually assumed to be the result of concentrations of elements by living organisms. For example, the data of Martin and Knauer (1973) indicate that plankton are enriched in Pb, Ni, Cu, Mn, Fe, and Zn. Holland (1979) suggested, however, that high concentrations of certain trace elements in organic-carbon-rich black shales may be more related to chemical precipitation and reaction with organic detritus under anoxic conditions than to incorporation into living organisms. Unfortunately, it is not possible to separate the effects of chemical precipitation and bioconcentration, especially in anoxic, organic-carbon-rich strata. Both processes may have contributed to high concentrations of some trace elements in the organic-carbon-rich limestones in Unit II, Hole 465A, and in Unit III, Hole 463.



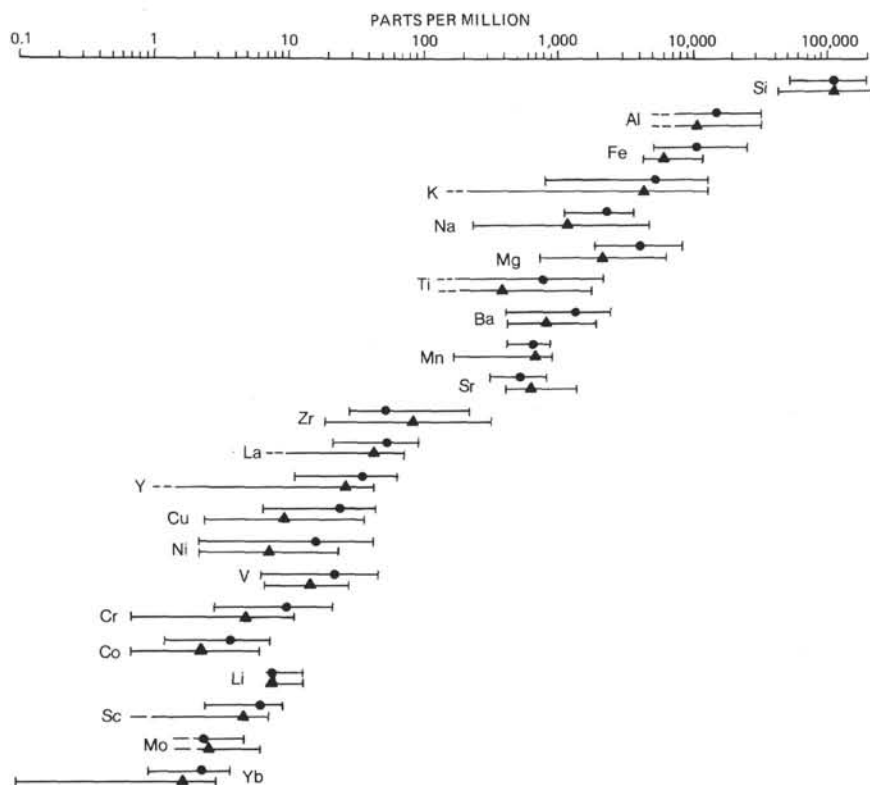


Figure 3. Comparison of element concentrations in 18 samples of red limestone (dots) and 16 samples of green limestone (triangles) from Lithologic Unit II, Hole 463. Dots and triangles represent the mean concentration for each element (Table 2). Bars indicate observed ranges of element concentrations (Table 2). A dash at the lower end of a bar indicates that the lowest concentration of the element was below the limit of detection.

Extreme variations in element concentrations in samples of olive-gray laminated limestone immediately overlying trachyte in Core 40 are evident in Figure 5 and Table 5, and are discussed by Dean et al. in their paper on geochemistry of rocks above basement at Site 465 (this volume). These samples were not included in the summary statistics for olive laminated limestone in Figure 7 and Table 6.

#### Site 466

Results of analyses of 33 samples (including five analytical duplicates) from Hole 466 are given in Table 7 and plotted versus sub-bottom depth in Figure 8. Because of the abundance of chert below about 84 meters sub-bottom, the only lithologic units that could be adequately sampled in Hole 466 were Unit IA and the top of Unit IB. Both units consist mainly of white nanofossil ooze. Unit IA contains higher concentrations of impurities, as indicated by common gray and brown zones and higher concentrations of siliceous microfossils, clay, zeolites, hematite, and volcanic glass (as observed in smear slides), relative to nanofossil oozes from Unit IB and those from Sites 463 and 465 (see lithologic descriptions in site chapters, this volume).

Most samples from Unit IA contain between 70 and 90%  $\text{CaCO}_3$ , whereas all samples from Unit IB contain more than 90%  $\text{CaCO}_3$ .

Higher concentrations of impurities in Unit IA are further reflected by higher and more-variable concentrations of most elements. Summary statistics of element concentrations in nanofossil ooze and chalk from Sites 463, 465, and 466 are presented in Table 8 and plotted in Figure 9. Higher concentrations of most elements in ooze from Hole 466 are evident from Table 8; differences are most noticeable for Fe, Na, Ti, Co, Cu, Mn, Mo, Ni, V, and Zr.

Unit II consists of olive-gray chalk and limestone containing up to 8.1% organic carbon; these are equivalent to the organic-carbon-rich, olive laminated limestone of Unit II, Hole 465A. Unfortunately, recovery of the rocks in Unit II was so poor that not enough samples could be collected to characterize the geochemistry of this unit.

#### ACKNOWLEDGMENTS

I am grateful to J. R. Herring and J. M. McNeal for helpful reviews of the manuscript. G. H. Harrach provided valuable assistance with computer graphics for the down-hole plots of element concentration.

Table 3. Chemical analyses of samples from Hole 464.

Sample	Site-Core-Section, Interval (cm)	Sub-bottom Depth (m)	SiO <sub>2</sub> -S	SiO <sub>2</sub> -xrf	Al <sub>2</sub> O <sub>3</sub> -S	Al <sub>2</sub> O <sub>3</sub> -xrf	Fe <sub>2</sub> O <sub>3</sub> -S	Fe <sub>2</sub> O <sub>3</sub> -xrf	MgO-sw	CaO-S	CaO-xrf	Na <sub>2</sub> O-sw	K <sub>2</sub> O-S	K <sub>2</sub> O-xrf	TiO <sub>2</sub> -S	TiO <sub>2</sub> -xrf
			(%)	(%)	(%)	(%)	(%)	(%)	(%)	(%)	(%)	(%)	(%)	(%)	(%)	(%)
40022070	464-2-2, 70	5.70	27.8	50	3.40	9.6	2.14	3.80	1.79	4.48	12.0	1.7270	2.05	2.30	0.138	0.40
40022071	464-2-2, 70	5.70	34.2	50	4.72	9.6	2.86	3.80	2.00	6.72	12.0	0.7019	2.41	2.30	0.285	0.40
40032138	464-3-2, 138	14.38	36.4	55	4.16	7.7	2.14	2.70	1.51	6.72	12.0	0.3023	2.17	1.90	0.210	0.30
40042070	464-4-2, 70	24.70	38.5	56	7.37	12.0	4.29	5.30	2.29	2.38	2.9	0.7525	3.37	2.90	0.300	0.53
40052020	464-5-2, 20	33.70	36.4	55	6.99	13.0	4.43	5.70	2.13	1.08	1.2	0.9777	3.01	3.00	0.270	0.58
40052021	464-5-2, 21	33.70	6.2	55	1.89	13.0	0.80	5.90	2.29	32.18	1.2	0.6525	0.42	3.00	0.113	0.60
40062082	464-6-2, 82	43.82	32.1	50	9.26	17.0	6.72	11.00	2.70	1.54	1.9	2.9510	5.54	4.20	0.465	1.40
40062083	464-6-2, 82	43.82	27.8	50	6.42	16.0	5.72	11.00	2.61	1.32	1.9	0.8259	4.34	4.20	0.390	1.40
40072010	464-7-2, 10	51.10	30.0	49	6.80	13.0	8.58	14.00	3.22	0.67	0.7	1.2264	5.18	4.30	0.615	2.30
40082040	464-8-2, 40	62.40	27.8	48	5.29	13.0	7.29	13.00	2.81	1.40	1.4	1.2514	6.99	5.40	0.495	1.90
40091110	464-9-1, 110	71.10	9.0	49	1.38	13.0	22.88	14.00	1.97	1.05	0.6	0.1771	0.89	4.40	0.053	2.30
40102070	464-10-2, 70	81.70	34.2	53	4.53	10.0	4.72	6.80	0.02	3.36	6.0	0.0001	2.53	2.70	0.210	0.50
40102071	464-10-2, 70	81.74	>72.7	95	0.38	2.0	0.53	0.30	2.92	0.77	1.1	1.2009	0.18	0.20	<0.010	<0.05
40111071	464-11-1, 71	89.71	>72.7	86	0.53	2.0	0.56	0.50	0.43	4.06	8.0	0.1176	0.28	0.30	0.017	0.06
40138009	464-13-8, 9	108.09	47.1	69	0.28	1.0	0.64	0.79	0.57	4.34	17.0	0.0951	0.28	0.45	0.013	<0.05

Note: Analyses were by X-ray fluorescence (xrf), semiquantitative optical emission spectroscopy (S), or atomic absorption (aa); analytical values for Mg and Na by atomic absorption were corrected for interstitial sea water (sw; see text for method of correction).

## REFERENCES

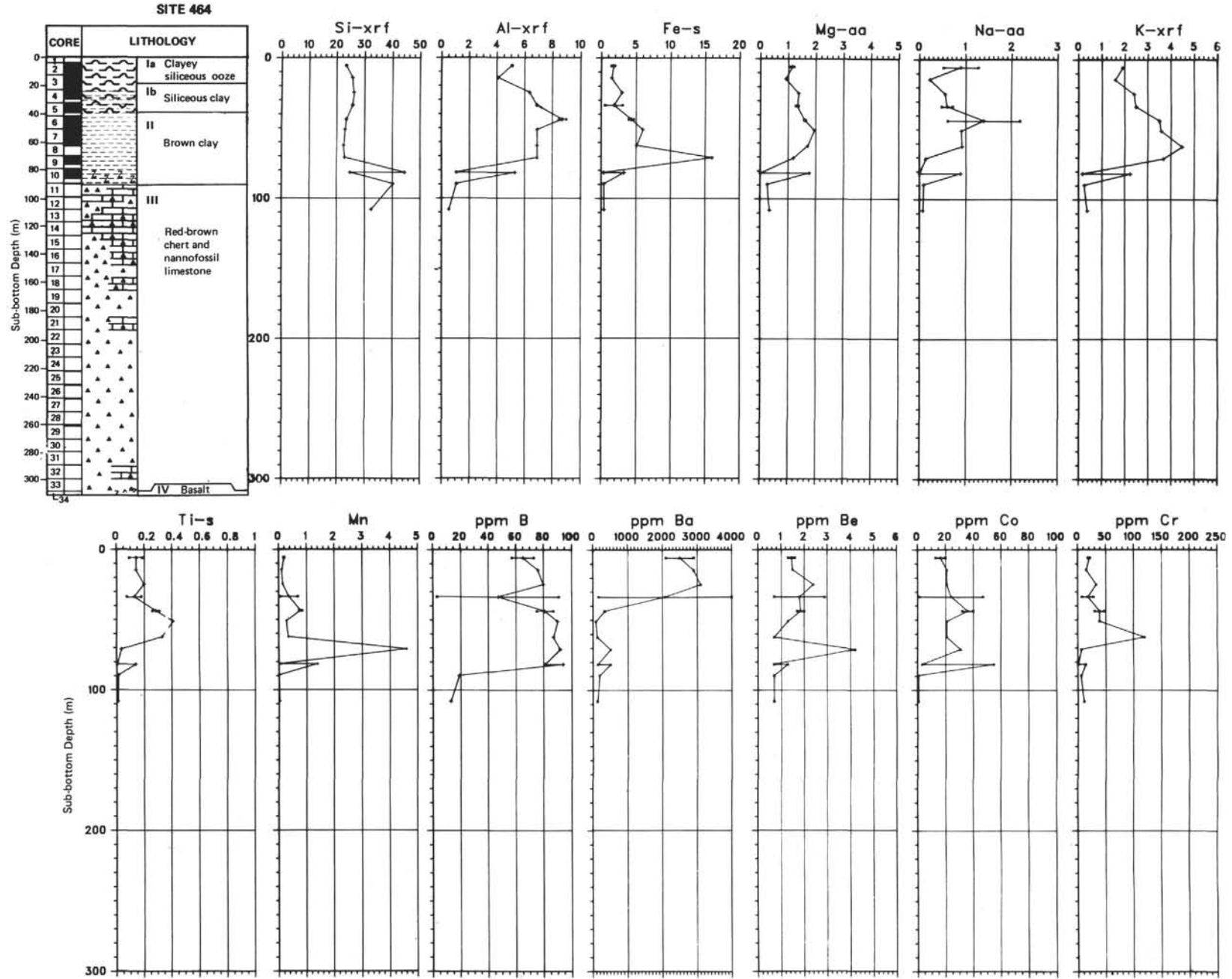
- Brongersma-Sanders, M., 1965. Metals of Kupferschiefer supplied by normal seawater. *Geol. Rundschau*, 55:365-375.
- Burns, R. G., and Brown, B. A., 1972. Nucleation and mineralogical controls on the composition of manganese nodules. In Horn, D. R. (Ed.), *Ferromanganese Deposits on the Ocean Floor*: Washington (National Science Foundation), pp. 51-61.
- Burns, R. G., and Burns, V. M., 1977. Mineralogy. In Glasby, G. P. (Ed.), *Marine Manganese Deposits*: Amsterdam (Elsevier), pp. 185-248.
- Calvert, S. E., and Price, N. B., 1970. Minor metal contents of recent organic-rich sediments off South West Africa. *Nature*, 227: 593-595.
- Chester, R., Griffiths, A., and Stoner, J. H., 1978. Minor metal content of surface seawater particulates and organic-rich shelf sediments. *Nature*, 275:308-309.
- Holland, H. D., 1979. Metals in black shales—a reassessment. *Econ. Geol.*, 74:1676-1680.
- Martin, J. H., and Knauer, G. A., 1973. The elemental composition of plankton. *Geochim. Cosmochim. Acta*, 37:1639-1653.
- Miesch, A. T., 1976. Geochemical survey of Missouri—methods of sampling, laboratory analysis, and statistical reduction of data. *U.S. Geol. Survey Prof. Paper*, 954-A.
- Turekian, K. K., 1964. The marine geochemistry of strontium. *Geochim. Cosmochim. Acta*, 28:1479-1496.
- Varentsov, I. M., and Pronina, N. V., 1973. On the study of mechanisms of iron-manganese ore formation in Recent basins: the experimental data on nickel and cobalt. *Mineral Deposita*, 8:161-178.
- Vine, J. D., and Tourtelot, E. B., 1970. Geochemistry of black shale deposits—a summary report. *Econ. Geol.*, 65:253-272.
- Volkov, I. I., and Fomina, L. S., 1974. Influence of organic materials and processes of sulfide formation on distribution of some trace elements in deep-water sediments of Black Sea. In Degens, E. T., and Ross, D. A. (Eds.), *The Black Sea—Geology, Chemistry, and Biology*: Am. Assoc. Petrol. Geol. Mem., 20:457-476.
- Wangersky, P. J., and Joensuu, Oiva, 1964. Strontium, magnesium, and manganese in fossil foraminifer carbonates. *J. Geol.*, 72:477-483.
- , 1967. The fractionation of carbonate deep-sea cores. *J. Geol.*, 75:148-177.
- Wedepohl, K. H., 1964. Untersuchungen am Kupferschiefer in Nord-west deutschland; ein Beitrag zur Deutung der Genese bituminöser Sediment. *Geochim. Cosmochim. Acta*, 28:305.

Table 3. (Continued).

B-S (ppm)	Ba-S (ppm)	Be-S (ppm)	Co-S (ppm)	Cr-S (ppm)	Cu-S (ppm)	Ga-S (ppm)	La-S (ppm)	Li-aa (ppm)	Mn-S (ppm)	Mo-S (ppm)	Ni-S (ppm)	Pb-S (ppm)	Rb-aa (ppm)	Sc-S (ppm)	Sn-S (ppm)	Sr-S (ppm)	V-S (ppm)	Y-S (ppm)	Yb-S (ppm)	Zn-S (ppm)	Zr-S (ppm)
57.0	2,100	1.3	13.0	18.0	58.0	12.0	26	37	1,800	<2.2	83.0	12.0	65	10.0	1.6	430	49.0	20.0	2.30	110	80.0
73.0	2,900	1.6	20.0	22.0	77.0	16.0	42	37	2,100	<2.2	110.0	15.0	67	15.0	2.1	690	69.0	29.0	3.40	93	110.0
76.0	2,900	1.5	21.0	15.0	48.0	12.0	31	31	1,100	<2.2	95.0	17.0	51	14.0	2.0	660	42.0	21.0	2.60	65	68.0
80.0	3,100	2.4	21.0	33.0	97.0	22.0	50	46	1,500	<2.2	110.0	19.0	69	18.0	3.7	380	83.0	39.0	4.10	72	150.0
91.0	>3,200	2.9	47.0	28.0	90.0	18.0	54	61	6,900	<2.2	170.0	22.0	100	18.0	3.8	350	75.0	51.0	4.60	71	140.0
<4.6	160	<1.0	1.3	7.8	3.1	3.3	58	58	350	5.0	4.5	<6.8	80	4.0	<1.5	550	50.0	11.0	1.10	<10	220.0
87.0	350	2.0	40.0	48.0	260.0	19.0	73	55	8,500	8.6	150.0	31.0	87	19.0	<1.5	210	84.0	79.0	11.00	110	90.0
75.0	330	1.7	32.0	30.0	220.0	15.0	63	48	7,300	8.4	110.0	110.0	68	17.0	<1.5	160	73.0	74.0	8.60	95	120.0
90.0	87	1.3	21.0	39.0	70.0	11.0	23	55	2,800	<2.2	68.0	<6.8	43	15.0	<1.5	92	55.0	21.0	2.40	99	66.0
87.0	130	<1.0	21.0	120.0	96.0	12.0	21	48	3,500	<2.2	80.0	<6.8	53	11.0	<1.5	89	61.0	19.0	2.90	83	53.0
92.0	510	4.2	31.0	6.2	890.0	5.9	180	18	46,000	74.0	150.0	75.0	25	10.0	<1.5	520	200.0	98.0	8.60	350	150.0
94.0	510	1.3	55.0	14.0	400.0	10.0	260	67	14,000	2.6	170.0	20.0	53	24.0	5.6	330	42.0	220.0	21.00	210	87.0
81.0	140	<1.0	3.4	<1.0	34.0	<1.5	15	12	780	<2.2	11.0	<6.8	<10	1.7	<1.5	19	5.8	18.0	1.20	18	11.0
19.0	190	<1.0	<1.0	6.0	7.7	<1.5	<10	13	77	<2.2	3.3	<6.8	<10	1.4	<1.5	120	5.3	5.3	0.42	22	7.1
13.0	130	<1.0	<1.0	11.0	59.0	<1.5	<10	10	370	<2.2	9.0	<6.8	<10	1.8	<1.5	240	7.3	7.3	0.56	44	14.0

Table 4. Summary statistics for element concentrations in 12 samples of brown clay from Lithologic Unit II, Hole 464.

Element	Observed Range	Arithmetic Mean	Standard Deviation
Si (%)	2.9-18	13	4.9
Al	4.1-8.9	6.5	1.4
Fe	0.56-16	4.2	4.0
Mn	0.35-4.6	0.80	1.3
Mg	0.11-0.34	0.22	0.084
Ca	0.43-8.6	3.2	3.4
Na	0.89-2.8	1.9	0.70
K	1.6-4.5	2.8	0.89
Ti	0.035-0.41	0.20	0.11
B (ppm)	3.0-94	75	25
Ba	87-4000	140	150
Be	0.70-4.2	1.8	0.98
Co	13-55	27	15
Cr	6.2-120	32	31
Cu	3.1-890	190	250
Ga	3.3-22	13	5.6
La	21-260	73	73
Li	18-67	47	14
Mo	1.5-74	9.1	21
Ni	4.5-170	110	48
Pb	5.0-110	28	32
Rb	25-100	63	20
Sc	4.0-24	15	5.3
Sr	89-690	370	210
V	42-200	74	43
Y	11-220	57	59
Yb	1.1-21	6.3	5.8
Zn	7.0-350	110	88
Zr	53-220	110	48



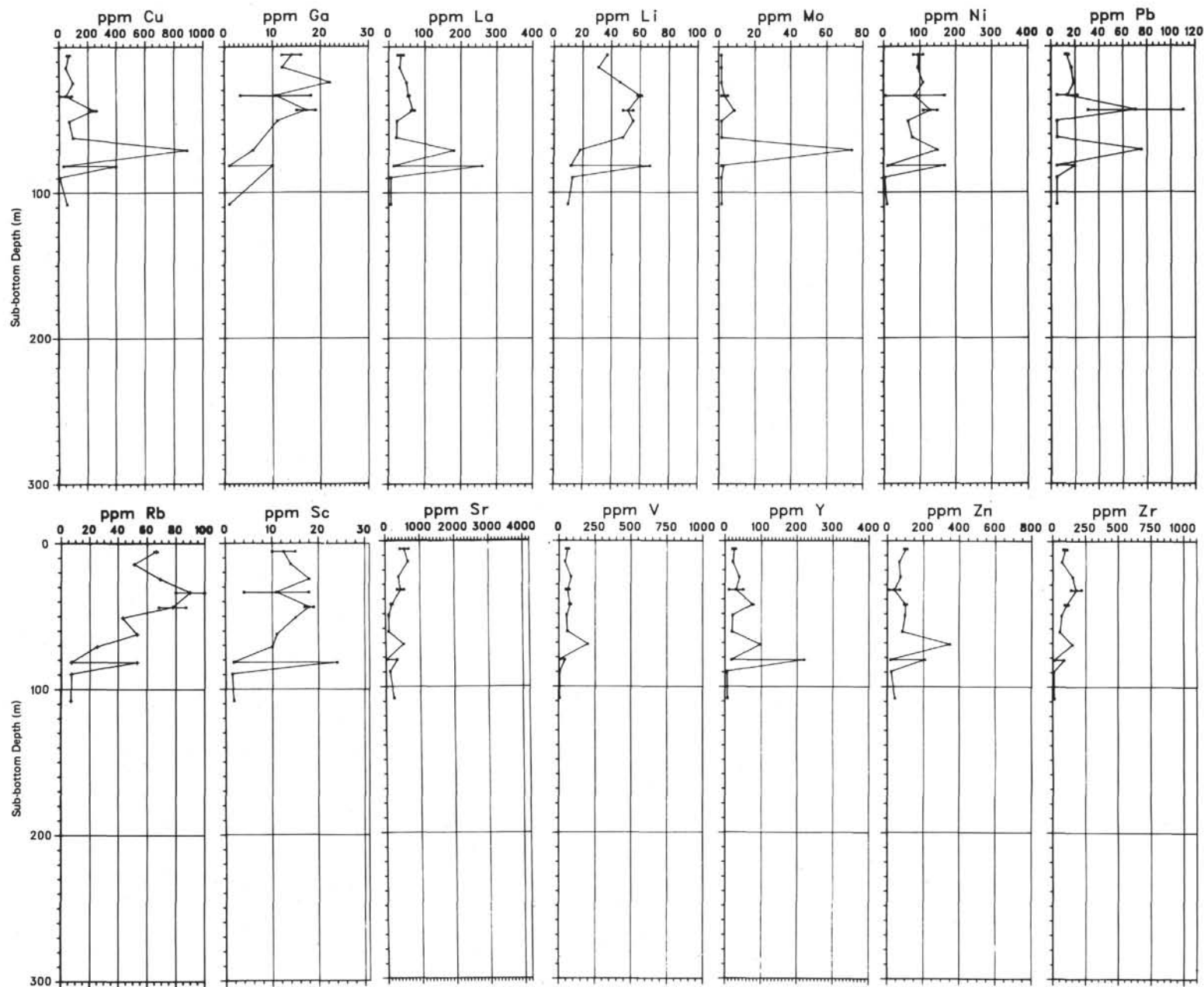
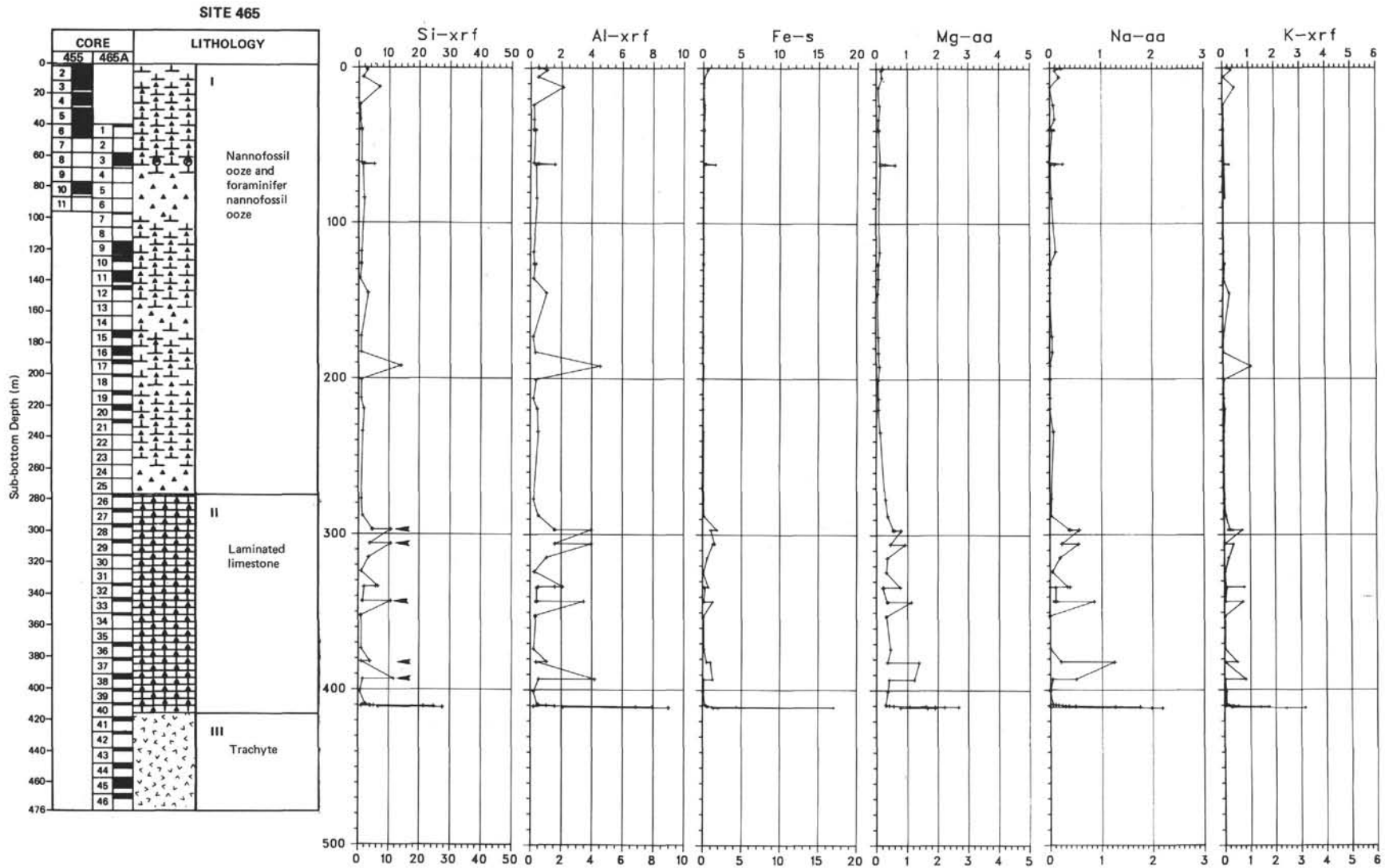


Figure 4. Lithologic summary and plots of element concentrations in samples from Hole 464. Element concentrations are in percent (unlabeled) or parts per million (labeled ppm) dry weight. Analyses were by X-ray fluorescence (xrf), semiquantitative optical emission spectroscopy (s), or atomic absorption spectrophotometry (aa). Duplicate analyses are indicated by two points connected by a horizontal bar at the same depth. The thickness of the black interval beside each core number in the column labeled "core" indicates the proportion of the cored interval that was recovered.









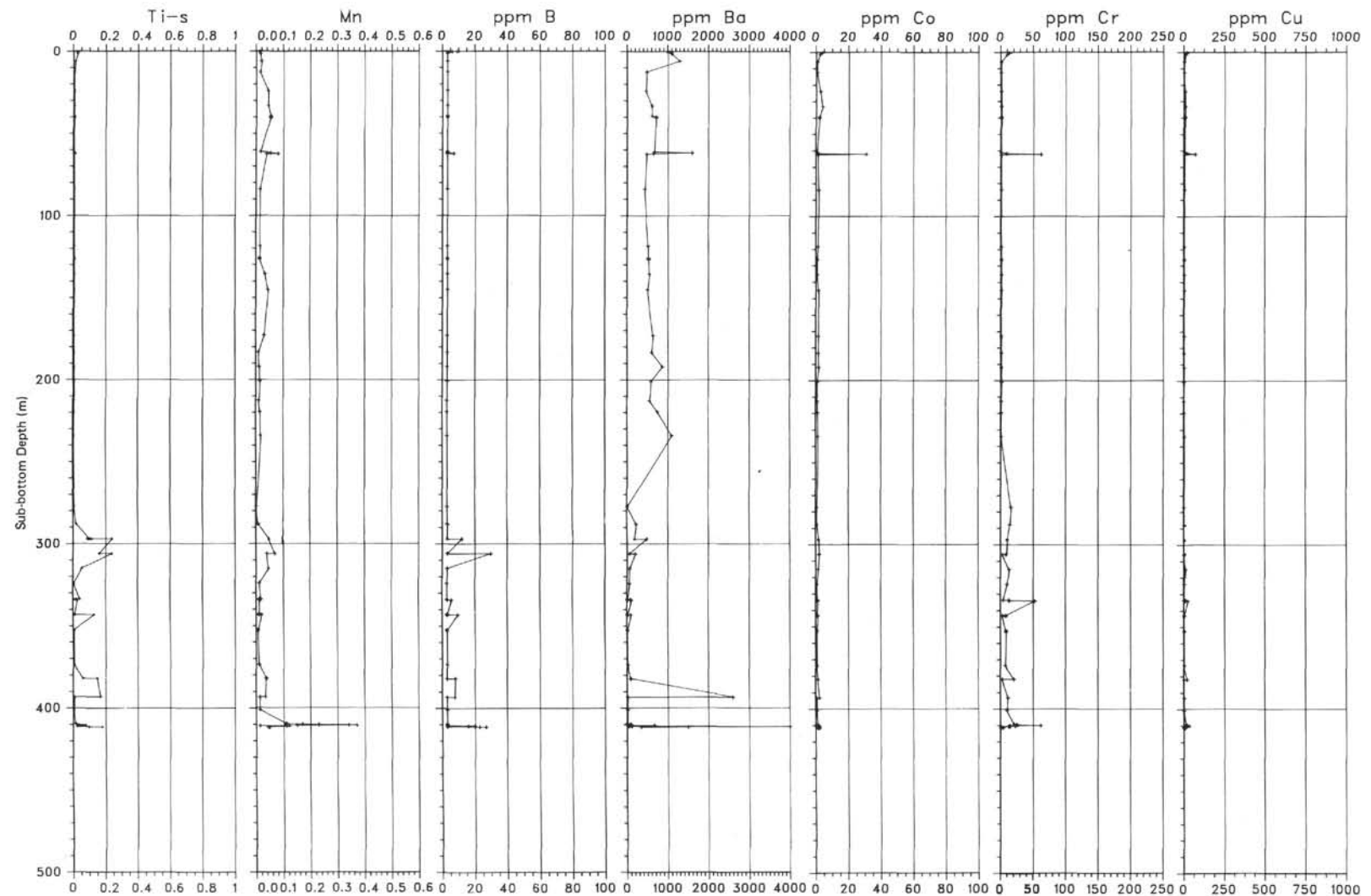


Figure 5. Lithologic summary and plots of element concentrations in samples from Holes 465 and 465A. Element concentrations are in percent (unlabeled) or parts per million (labeled ppm) dry weight. Analyses were by X-ray fluorescence (xrf), semiquantitative optical emission spectroscopy (s), or atomic absorption spectrophotometry (aa). Duplicate analyses are indicated by two points connected by a horizontal bar at the same depth. The thickness of the black interval beside each core number in the column labeled "core" indicates the proportion of the cored interval that was recovered. Arrows by concentrations of Si in five samples from Unit II indicate samples of gray limestone that are interbedded with olive laminated limestone.

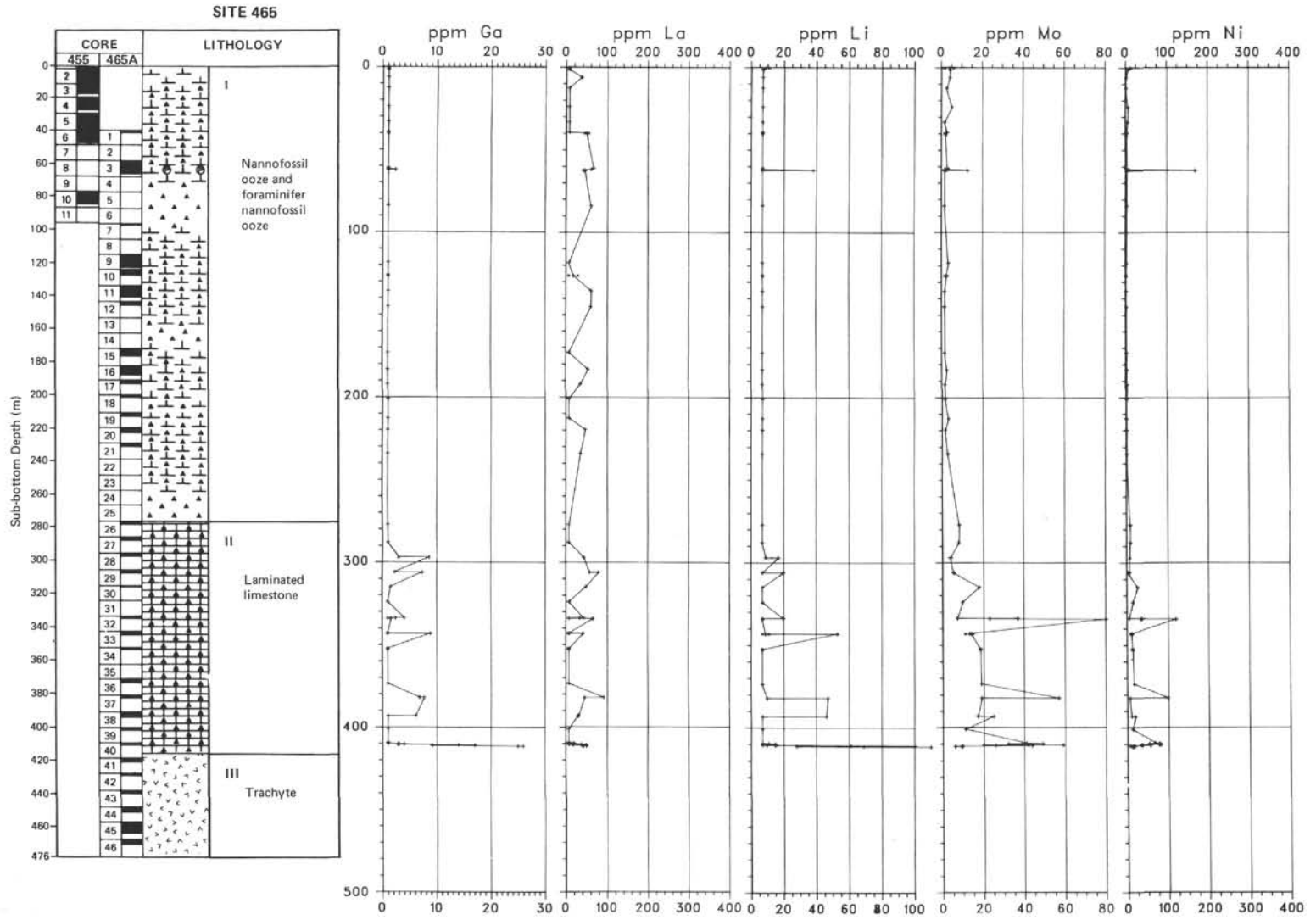


Figure 5. (Continued).

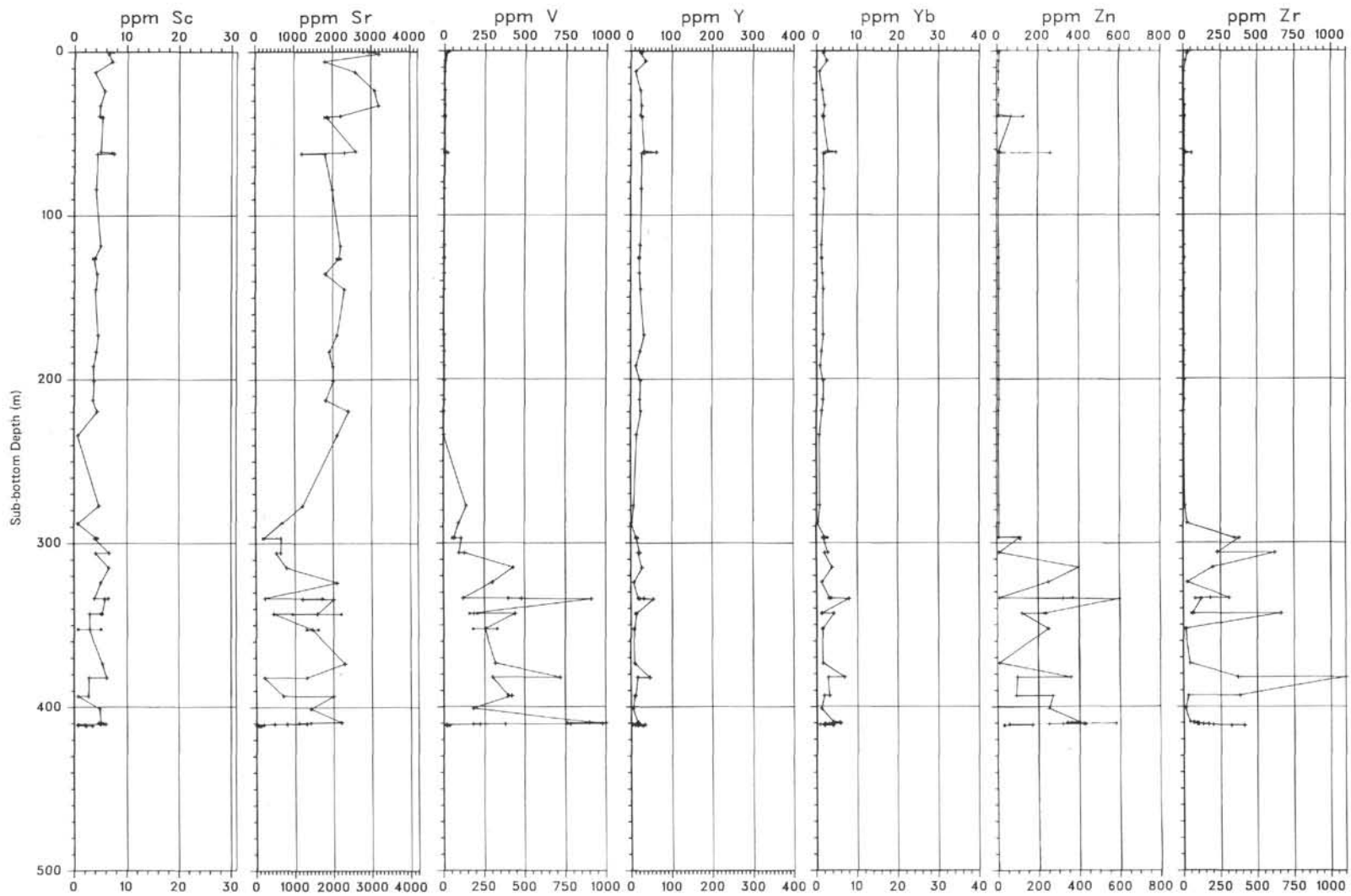


Figure 5. (Continued).

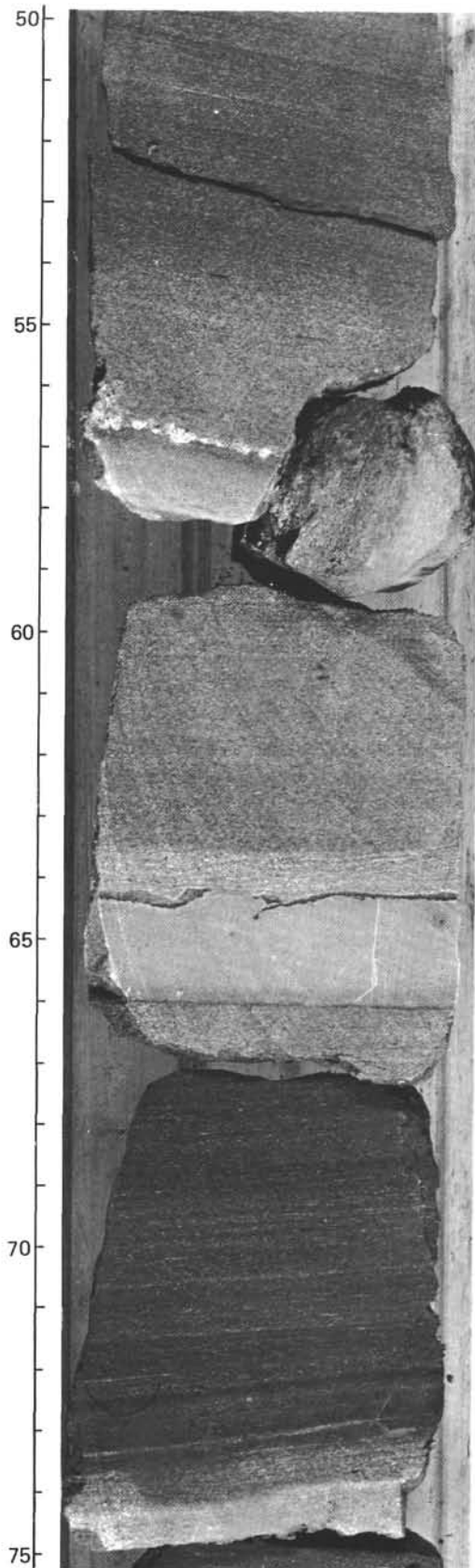


Table 6. Summary statistics for total element concentrations in 24 samples of olive laminated limestone and five samples of gray massive limestone from Lithologic Unit II, Hole 465A.

Element	Olive Laminated Limestone			Gray Massive Limestone		
	Observed Range	Arithmetic Mean	Standard Deviation	Observed Range	Arithmetic Mean	Standard Deviation
Si (%)	0.47-6.5	2.6	1.7	0.94-12	9.0	4.5
Al	0.21-2.1	0.83	0.59	0.37-4.2	3.2	1.6
Fe	0.046-1.6	0.34	0.34	1.0-1.3	1.2	0.14
Mg	0.24-1.9	0.50	0.40	0.80-1.4	1.1	0.23
Na	0.0001-0.42	0.15	0.14	0.50-1.2	0.75	0.31
K	<0.017-0.78	0.15	0.20	<0.017-0.83	0.53	0.33
Ti	<0.013-0.16	0.033	0.038	0.13-0.24	0.19	0.051
Ba (ppm)	8-230	56	58	99-2600	700	110
Co	<0.7-1.9	1.0	0.38	1.3-2.5	1.8	0.60
Cr	3.6-62	18	15	2.7-12	5.1	4.6
Cu	1.6-34	9.2	9.1	<1.0-3.1	1.9	0.90
La	<7.0-92	25	25	31-79	49	21
Li	<7.0-20	8.9	3.4	17-53	37	17
Mn	22-3700	700	1100	200-470	350	99
Mo	<1.5-80	24	19	5.2-19	14	6.1
Ni	4.5-120	36	34	3.6-11	8.0	3.7
Sc	<0.70-6.7	4.5	1.9	2.7-4.2	3.3	0.66
Sr	190-2300	1300	600	210-700	500	190
V	55-1000	430	310	110-440	280	150
Y	1.0-55	17	13	11-18	14	2.7
Yb	0.30-8.0	3.0	2.0	1.8-4.2	2.8	0.97
Zr	11-370	110	110	380-1100	630	290

Figure 6. Thin bed of gray massive limestone in olive laminated limestone from Lithologic Unit II, Hole 465A, Core 36, Section 2, 50 to 75 cm. Subdivisions on scale are in millimeters.

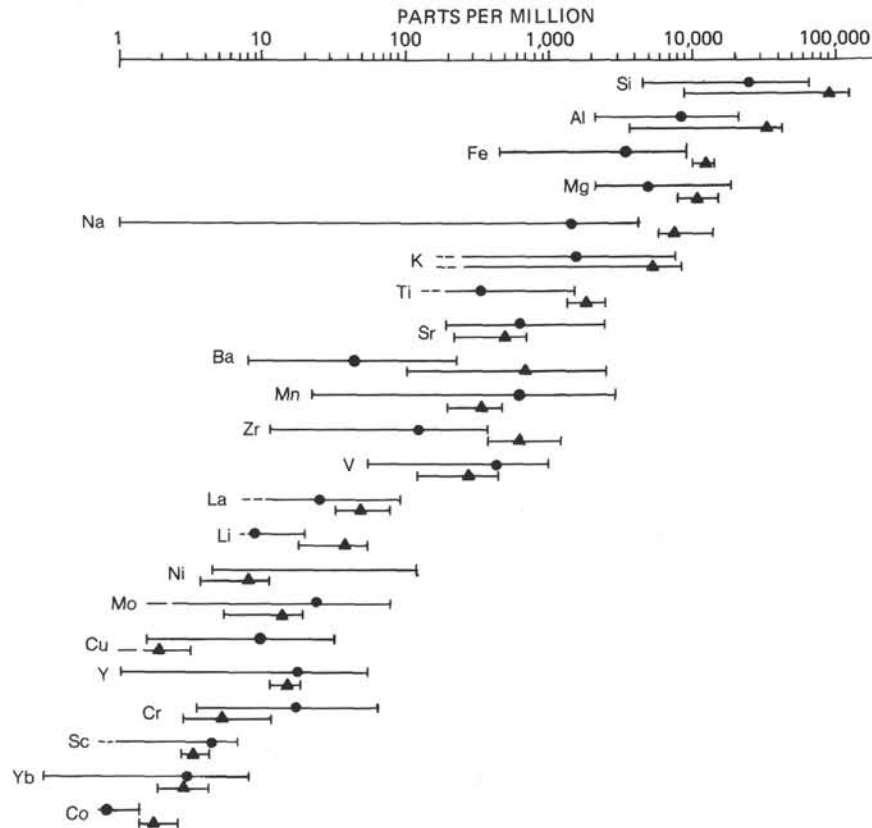


Figure 7. Comparison of element concentrations in 25 samples of olive laminated limestone (dots) and five samples of gray massive limestone (triangles) from Lithologic Unit II, Hole 465A. Dots and triangles represent the mean concentration for each element (Table 6). Bars indicate observed ranges of element concentrations (Table 6). A dash at the lower end of a bar indicates that the lowest concentration of the element was below the limit of detection.

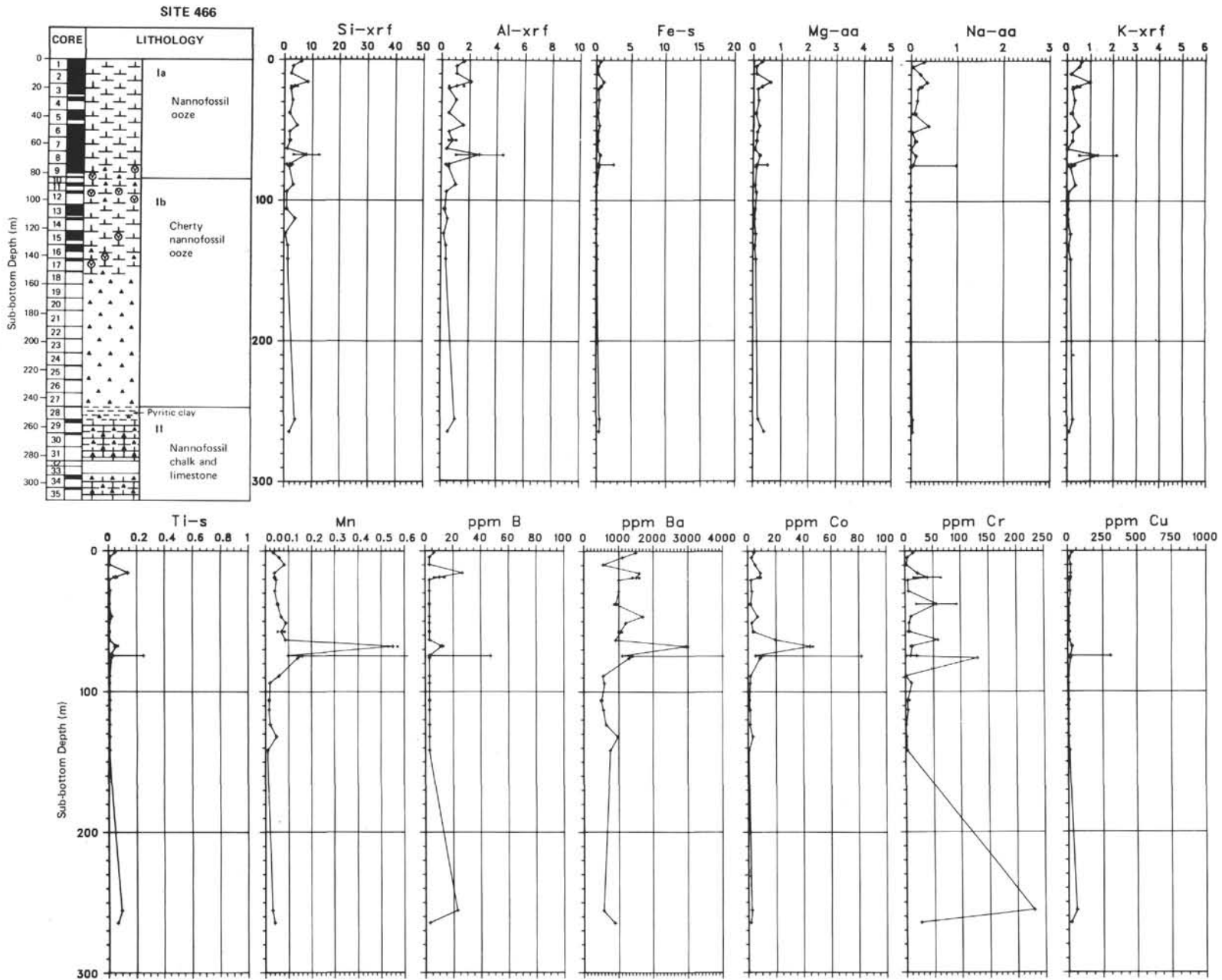
Table 7. Chemical analyses of samples from Hole 466.

Sample	Site-Core-Section, Interval (cm)	Sub-bottom Depth (m)	SiO <sub>2</sub> -S	SiO <sub>2</sub> -xrf	Al <sub>2</sub> O <sub>3</sub> -S	Al <sub>2</sub> O <sub>3</sub> -xrf	Fe <sub>2</sub> O <sub>3</sub> -S	Fe <sub>2</sub> O <sub>3</sub> -xrf	MgO-swc	CaO-S	CaO-xrf	Na <sub>2</sub> O-swc	K <sub>2</sub> O-S	K <sub>2</sub> O-xrf	TiO <sub>2</sub> -S
			(%)	(%)	(%)	(%)	(%)	(%)	(%)	(%)	(%)	(%)	(%)	(%)	(%)
60011130	466-1-1, 130	1.32	5.35	13.0	1.57	3.0	0.872	0.92	0.508	28	52	0.3756	0.78	0.75	0.072
60014020	466-1-4, 20	4.70	1.33	6.5	0.30	2.0	0.372	0.58	0.168	35	56	0.0456	0.39	0.64	0.012
60022036	466-2-2, 36	9.86	1.48	5.0	0.25	2.0	0.372	0.09	0.198	31	61	0.2756	0.35	0.20	<0.010
60026032	466-2-6, 32	15.82	11.98	18.0	3.59	4.0	1.573	1.30	1.033	36	46	0.4758	1.16	1.20	0.210
60031137	466-3-1, 137	18.87	6.85	5.2	1.89	1.0	0.987	0.08	0.506	>45	62	0.3257	0.84	0.30	0.093
60031138	466-3-1, 137	18.87	4.49	10.0	1.42	3.0	0.886	0.77	0.524	31	55	0.2507	0.78	0.66	0.057
60033023	466-3-3, 23	20.73	1.67	5.0	0.30	1.0	0.458	0.20	0.267	34	62	0.2006	0.36	0.30	<0.010
60042008	466-4-2, 8	28.58	1.84	6.4	0.45	2.0	0.572	0.30	0.321	27	59	0.1855	0.48	0.41	0.015
60051130	466-5-1, 130	37.80	0.92	4.0	0.23	1.0	0.343	<0.05	0.178	29	63	0.1556	0.35	0.30	<0.010
60051131	466-5-1, 130	37.80	0.66	4.0	0.21	1.0	0.315	<0.05	0.156	31	63	0.0257	0.33	0.20	<0.010
60061073	466-6-1, 73	46.73	2.57	10.0	0.87	3.0	0.686	0.79	0.376	32	55	0.5257	0.55	0.62	0.035
60064073	466-6-4, 73	51.23	0.96	4.0	0.28	1.0	0.386	0.06	0.239	29	62	0.0505	0.39	0.30	<0.010
60072040	466-7-2, 40	57.40	1.37	4.0	0.32	1.0	0.443	0.09	0.216	35	62	0.1257	0.41	0.30	<0.010
60072041	466-7-2, 40	57.40	0.92	5.0	0.26	2.0	0.429	0.20	0.213	27	60	0.1758	0.42	0.30	<0.010
60076040	466-7-6, 40	63.40	0.39	2.0	0.09	0.7	0.200	<0.05	0.106	41	65	0.0001	0.24	<0.03	<0.010
60082130	466-8-2, 130	67.80	4.71	7.2	2.27	2.0	0.886	0.55	0.378	>45	57	0.1456	0.70	0.64	0.098
60082131	466-8-2, 130	67.80	4.28	27.0	1.62	8.4	0.844	4.20	0.440	39	27	0.1555	0.67	2.60	0.065
60091008	466-9-1, 8	74.58	0.73	4.0	0.21	1.0	0.415	0.10	0.222	32	62	0.0679	0.33	0.20	0.014
60091014	466-9-1, 14	74.64	15.83	2.0	4.72	0.6	3.574	<0.05	0.856	17	65	1.3257	3.01	0.06	0.375
60091024	466-9-1, 24	74.74	4.06	6.2	0.55	1.0	0.600	0.20	0.207	42	61	0.0001	0.42	0.40	0.041
60092022	466-9-2, 22	76.22	1.11	4.0	0.47	1.0	0.543	0.08	0.194	38	63	0.0001	0.39	0.20	0.024
60111094	466-11-1, 94	88.94	0.34	7.1	<0.06	2.0	0.087	0.40	0.129	>45	59	0.0001	0.20	0.45	<0.010
60121054	466-12-1, 54	94.04	0.28	2.0	<0.06	0.7	0.063	<0.05	0.207	38	64	0.0001	0.20	0.09	<0.010
60133015	466-13-3, 15	106.15	0.32	2.0	<0.06	<0.5	0.079	<0.05	0.121	32	64	0.0001	0.19	0.08	<0.010
60133016	466-13-3, 15	106.15	0.36	2.0	<0.06	0.6	0.071	<0.05	0.134	32	65	0.0001	0.19	0.04	<0.010
60141062	466-14-1, 62	113.12	4.06	8.7	<0.06	0.9	0.109	<0.05	0.097	>45	61	0.0001	0.20	0.06	<0.010
60152015	466-15-2, 15	123.65	0.13	1.0	<0.06	<0.5	0.026	<0.05	0.173	34	65	0.0180	<0.08	0.20	<0.010
60161060	466-16-1, 60	132.10	0.47	3.0	0.09	0.7	0.172	<0.05	0.122	>45	64	0.0001	0.24	0.09	<0.010
60171084	466-17-1, 84	141.84	0.47	3.0	<0.06	0.7	0.200	0.06	0.181	29	64	0.0104	0.30	0.20	<0.010
60291071	466-29-1, 71	255.71	6.42	8.6	1.51	2.0	0.701	0.20	0.319	41	49	0.0480	0.42	0.30	0.140
60301011	466-30-1, 11	264.61	1.65	4.0	0.60	1.0	0.529	0.08	0.668	41	63	0.0376	0.19	0.10	0.093
60341049	466-34-1, 49	293.49	5.13	—	0.70	—	0.400	—	0.341	42	—	0.0001	0.22	—	0.083
60351026	466-35-1, 26	302.76	4.06	6.4	0.98	1.0	0.615	0.20	0.262	41	57	0.0003	0.40	0.30	0.056

Note: Analyses were by X-ray fluorescence (xrf), semiquantitative optical emission spectroscopy (S), and atomic absorption (aa); analytical values for Mg and Na by atomic absorption were corrected for interstitial sea water (swc; see text for method of correction). Dashes indicate no analysis.

Table 7. (Continued).

TiO <sub>2</sub> -xrf (%)	B-S (ppm)	Ba-S (ppm)	Co-S (ppm)	Cr-S (ppm)	Cu-S (ppm)	Ga-S (ppm)	La-S (ppm)	Li-aa (ppm)	Mn-S (ppm)	Mo-S (ppm)	Ni-S (ppm)	Rb-aa (ppm)	Sc-S (ppm)	Sn-S (ppm)	Sr-S (ppm)	V-S (ppm)	Y-S (ppm)	Yb-S (ppm)	Zn-S (ppm)	Zr-S (ppm)
0.10	6.4	1,500	4.6	15.0	30.0	2.0	37	11	340	2.7	7.4	<10	6.3	<1.5	2,000	16.0	30	2.20	<10	44.0
<0.05	<4.6	1,100	2.7	4.1	13.0	<1.5	<10	<10	600	4.1	3.5	<10	4.8	<1.5	4,200	4.9	22	1.50	<10	15.0
<0.05	<4.6	550	5.5	2.6	22.0	<1.5	<10	<10	830	3.0	5.3	10	4.9	<1.5	3,100	6.4	14	0.84	<10	18.0
0.20	27.0	1,600	9.3	23.0	22.0	4.9	42	<10	390	2.9	25.0	26	11.0	<1.5	2,100	42.0	31	2.60	<10	89.0
<0.05	14.0	1,600	9.4	16.0	19.0	2.9	<10	11	420	<2.2	17.0	15	8.6	5.1	3,900	32.0	37	2.70	<10	69.0
0.08	6.3	1,400	7.3	65.0	22.0	1.8	40	12	390	3.8	16.0	15	7.5	<1.5	2,200	21.0	25	1.80	<10	39.0
<0.05	<4.6	1,000	2.3	5.1	15.0	<1.5	<10	<10	470	3.3	4.1	<10	4.6	<1.5	3,100	5.6	20	1.30	<10	15.0
<0.05	<4.6	1,000	3.1	6.4	17.0	<1.5	<10	<10	410	2.8	3.3	10	4.4	<1.5	3,300	11.0	22	1.50	<10	17.0
<0.05	<4.6	950	2.2	20.0	11.0	<1.5	<10	<10	520	3.6	8.3	10	<1.0	3.1	3,700	6.3	24	1.60	<10	15.0
<0.05	<4.6	870	1.6	93.0	6.9	<1.5	<10	<10	550	2.9	2.6	<10	4.6	<1.5	2,800	4.0	20	1.10	<10	10.0
0.08	<4.6	1,700	7.2	10.0	10.0	1.6	41	<10	690	<2.2	12.0	14	5.4	<1.5	3,400	9.6	31	1.90	<10	26.0
<0.05	<4.6	1,200	2.8	6.7	8.0	<1.5	37	<10	900	2.6	6.7	<10	4.3	<1.5	2,500	5.4	24	1.40	<10	16.0
<0.05	<4.6	1,100	3.9	5.4	10.0	<1.5	<10	<10	850	3.4	6.4	<10	5.3	<1.5	3,300	6.2	19	1.20	<10	13.0
<0.05	<4.6	1,000	4.3	8.9	11.0	<1.5	<10	<10	540	3.0	4.9	10	4.3	<1.5	3,200	5.6	22	1.40	<10	13.0
<0.05	<4.6	910	20.0	59.0	12.0	<1.5	<10	<10	880	<2.2	7.6	<10	6.3	<1.5	4,200	3.1	43	3.10	<10	14.0
0.06	13.0	3,000	47.0	13.0	32.0	<1.5	210	<10	5,700	10.0	91.0	14	17.0	<1.5	3,500	30.0	250	16.00	<10	120.0
0.66	11.0	2,900	43.0	9.9	30.0	<1.5	200	<10	5,300	8.4	82.0	10	15.0	<1.5	3,200	24.0	240	15.00	<10	100.0
<0.05	<4.6	1,100	5.4	9.2	18.0	<1.5	<10	<10	990	3.5	17.0	<10	5.5	<1.5	1,900	5.3	43	2.90	<10	20.0
<0.05	47.0	>3,200	82.0	21.0	310.0	8.8	370	19	12,000	33.0	400.0	37	31.0	<1.5	2,000	70.0	390	34.00	150	230.0
<0.05	<4.6	1,400	10.0	1.2	19.0	<1.5	55	<10	1,600	5.3	22.0	10	7.7	<1.5	2,300	9.9	63	3.70	<10	46.0
<0.05	<4.6	1,300	8.7	130.0	18.0	<1.5	56	<10	1,400	5.0	18.0	<10	6.6	<1.5	1,900	6.8	35	2.40	<10	27.0
<0.05	<4.6	550	1.8	<1.0	3.5	<1.5	<10	<10	590	3.5	2.3	<10	6.2	3.2	3,200	2.8	44	2.80	250	9.4
<0.05	<4.6	590	1.6	11.0	4.7	<1.5	<10	<10	190	3.0	1.6	<10	4.5	<1.5	2,000	2.4	24	1.40	<10	5.0
<0.05	<4.6	520	1.2	6.8	4.6	<1.5	<10	<10	170	<2.2	1.5	<10	4.9	<1.5	2,400	2.1	18	1.10	<10	5.5
<0.05	<4.6	490	<1.0	<1.0	5.5	<1.5	<10	<10	160	<2.2	<1.5	<10	4.4	<1.5	2,400	2.4	27	1.90	<10	5.8
<0.05	<4.6	570	1.7	4.6	3.3	<1.5	<10	<10	160	4.3	1.7	<10	6.0	<1.5	2,400	2.7	31	1.80	<10	8.3
<0.05	<4.6	650	1.5	<1.0	4.0	<1.5	55	<10	210	<2.2	<1.5	<10	5.2	<1.5	1,800	2.2	20	0.91	<10	6.5
<0.05	<4.6	980	3.6	1.8	5.5	<1.5	74	<10	490	<2.2	2.6	<10	6.5	<1.5	3,200	3.6	41	2.60	<10	8.2
<0.05	<4.6	760	<1.0	2.8	11.0	<1.5	<10	<10	100	2.4	<1.5	<10	3.8	<1.5	1,900	2.8	12	0.75	<10	5.6
0.10	23.0	560	2.6	230.0	59.0	<1.5	63	<10	310	39.0	260.0	10	8.5	<1.5	4,000	590.0	110	8.90	750	68.0
0.10	<4.6	890	1.7	26.0	18.0	<1.5	<10	<10	410	5.7	21.0	<10	5.6	<1.5	2,200	98.0	25	1.10	<10	38.0
—	<4.6	520	1.6	260.0	26.0	<1.5	<10	<10	190	7.7	32.0	<10	6.5	<1.5	2,900	130.0	40	2.10	270	49.0
<0.05	5.3	310	1.7	110.0	29.0	<1.5	<10	<10	110	13.0	66.0	<10	7.0	<1.5	3,700	150.0	50	3.30	330	45.0





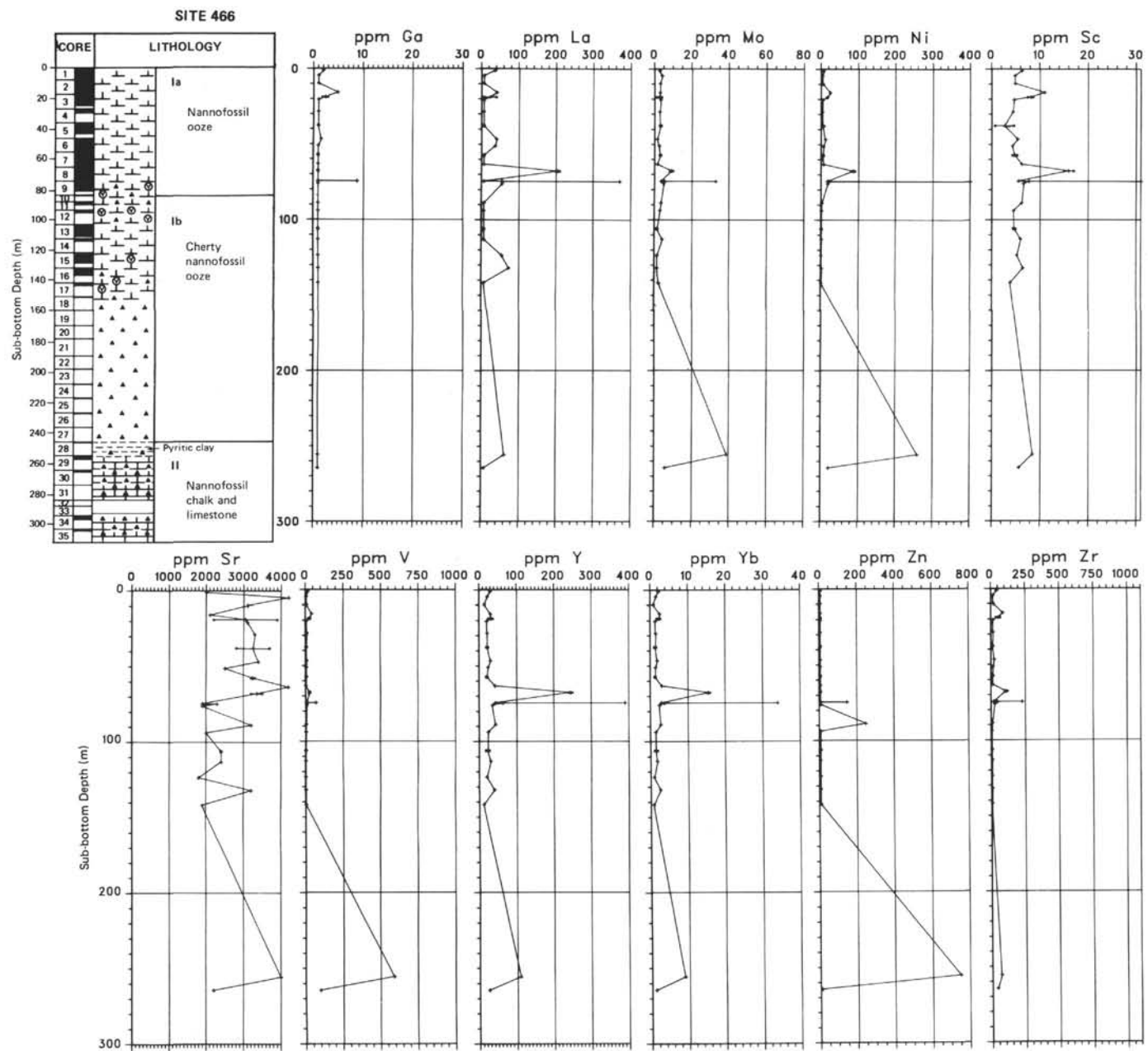


Figure 8. Lithologic summary and plots of element concentrations in samples from Hole 466. Element concentrations are in percent (unlabeled) or parts per million (labeled ppm) dry weight. Analyses were by X-ray fluorescence (xrf), semiquantitative optical emission spectroscopy (s), or atomic absorption spectrophotometry (aa). Duplicate analyses are indicated by two points connected by a horizontal bar at the same depth. The thickness of the black interval beside each core number in the column labeled "core" indicates the proportion of the cored interval that was recovered.

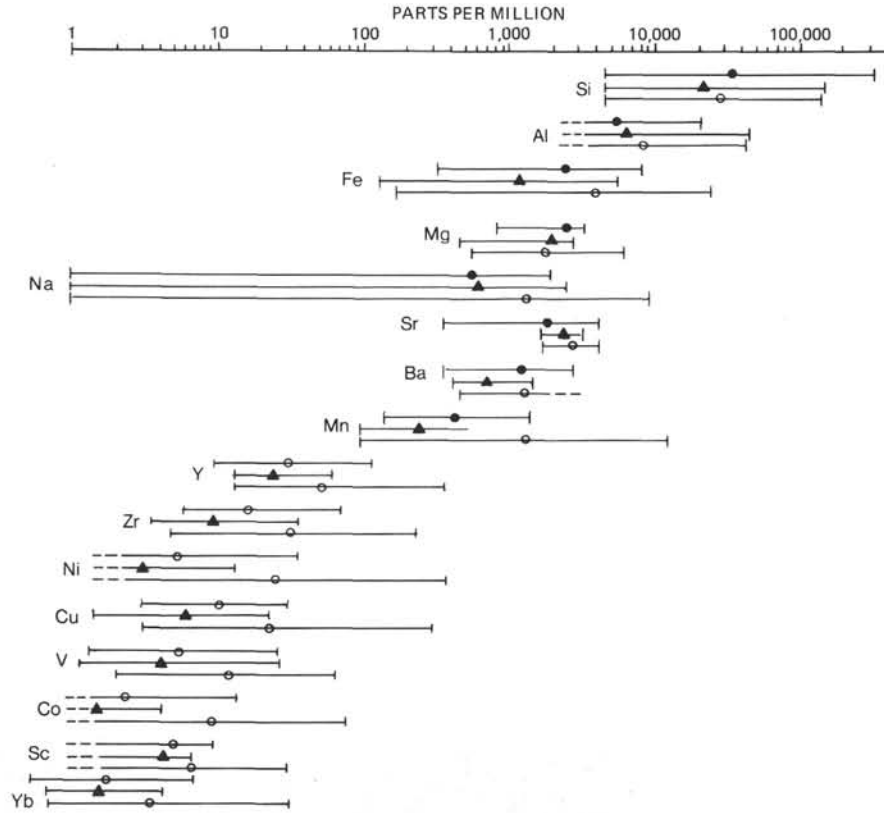


Figure 9. Comparison of element concentrations in 41 samples of nannofossil ooze and chalk from Lithologic Unit I, Hole 463 (dots); 25 samples of nannofossil ooze and chalk from Lithologic Unit I, Holes 465 and 465A (triangles); and 29 samples of nannofossil ooze from Lithologic Unit I, Hole 466 (open circles). Dots, triangles and open circles represent the mean concentration for each element (Table 8). Bars indicate observed ranges of element concentrations (Table 8). A dash at the lower end of a bar indicates that the lowest concentration of the element was below the limit of detection.

Table 8. Summary statistics for total element concentrations in 41 samples of nannofossil ooze and chalk from Lithologic Unit I, Hole 463; 25 samples of nannofossil ooze and chalk from Lithologic Unit I, Holes 465 and 465A; and 29 samples of nannofossil ooze from Lithologic Unit I, Hole 466.

Element	Hole 463			Holes 465 and 465A			Hole 466		
	Observed Range	Arithmetic Mean	Standard Deviation	Observed Range	Arithmetic Mean	Standard Deviation	Observed Range	Arithmetic Mean	Standard Deviation
Si (%)	0.47-34	3.4	5.5	0.47-14	2.1	2.8	0.47-13	2.9	2.5
Al	<0.26-2.1	0.55	0.34	<0.26-4.6	0.64	0.92	<0.26-4.4	0.87	0.84
Fe	0.032-0.81	0.26	0.18	0.013-0.58	0.12	0.17	0.018-2.5	0.40	0.47
Mg	0.088-0.32	0.16	0.054	0.047-0.29	0.10	0.060	0.058-0.62	0.18	0.13
Na	0.0001-0.20	0.057	0.051	0.0001-0.26	0.062	0.079	0.0001-0.98	0.13	0.20
K	<0.024-0.36	—	—	<0.024-1.1	—	—	<0.024-2.2	0.34	0.41
Ti	<0.006-0.077	—	—	<0.006-0.033	—	—	<0.006-0.25	—	—
Ba	0.039-0.28	0.12	0.049	0.043-0.16	0.074	0.030	0.049->0.32	0.125	0.080
Mn	0.014-0.14	0.045	0.029	0.0096-0.056	0.026	0.016	0.010-1.2	0.13	0.24
Sr	0.038-0.42	0.19	0.077	0.18-0.32	0.23	0.046	0.18-0.42	0.28	0.074
Co (ppm)	1.0-15	2.5	2.7	1.0-4.4	—	—	1.0-82	10	18
Cu	3.1-31	11	8.1	1.5-24	6.7	6.2	3.3-310	24	56
La	10-90	—	—	10-67	—	—	10-370	—	—
Mo	<2.2-8.3	—	—	<2.2-5.9	—	—	<2.2-33	—	—
Ni	<1.5-38	5.8	6.8	<1.5-13	—	—	<1.5-400	27	75
Sc	<1.0-9.9	5.2	2.0	<1.0-7.2	4.7	1.4	<1.0-31	7.1	5.6
V	1.4-28	6.0	5.8	1.2-29	4.4	6.6	2.1-70	12	15
Y	10-110	32	15	12-63	25	9.8	12-390	56	86
Yb	0.57-7.6	1.9	1.2	0.71-4.7	1.7	0.80	0.75-34	3.9	6.8
Zr	6.1-74	17	13	3.7-38	9.8	8.3	5.0-230	35	48